PNAS
www.pnas.org

Supplementary Information for

Centromere repositioning causes inversion of meiosis and generates a reproductive barrier

Min Lu, Xiangwei He*

Correspondence to: xhe@zju.edu.cn

This PDF file includes:

SI Materials and Methods

Figs. S1 to S9

Tables S1 to S5

References for SI reference citations

www.pnas.org/cgi/doi/10.1073/pnas.1911745116

SI Materials and Methods

Strain Constructions. All *S. pombe* strains used in this study are listed in SI Appendix, Table S5. Single inner kinetochore deletion strains (e.g., *fta6*Δ, *cnp3*Δ and *mhf2*Δ) are from the commercial Bionner *S. pombe* deletion library (1). The double-mutant *cnp3*Δ*fta6*Δ strains were obtained from genetic crossing between *fta6*Δ and *cnp3*Δ. The strains carrying both a neocentromere (or Cnp1 spreading) and the *otr1R::ura4* marker were obtained by crossing the *otr1R::ura4* marker strains (strain SPT999a or SPKY10) with strains carrying different neocentromeres (*mhf2*$^+$*cen2*$^{\text{inactive}}$, *mhf2*Δ*cen1*$^{\text{inactive}}$ or *mhf2*$^+$*cen1*$^{\text{inactive}}$). Construction of heterozygous gene deletion diploid strains and recovery of their meiotic haploid progeny were performed following standard procedures (2).

Chromatin Immunoprecipitation (ChIP). The procedure was performed as described previously (3). Anti-H3K9me2 (ab1220, Abcam) and anti-Cnp1 (gift from Robin Allshire, U. Edinburgh) antibodies were used for immunoprecipitation. Unless specified, yeast cells were cultured in YES medium at 29°C and harvested in the log phase. Temperature sensitive (*ts*) strains were cultured at 26°C (labeled as 26°C), or cultured at 26°C and then shifted to 36°C for 6 hours (labeled as 36°C). Biological replicates (labeled as "#") were performed in several indicated strains by H3K9me2 and Cnp1 ChIP-seq. Other ChIP-seq experiments were performed once.

High throughput sequencing and data analysis. The commercial library preparation kit (KAPA) and manufacturer's procedures were used for ChIP-seq library construction. Briefly, the DNA libraries were sequenced on the Ion PGM$^{\text{TM}}$ system (Life Technologies). Raw reads were aligned to the assembly *S. pombe* genome ASM294v.2.22 using Burrows-Wheeler Aligner (BWA)'s default parameters, which randomly assigned the ChIP-seq reads to the repetitive DNA sequences. Model-based Analysis of ChIP-seq (MACS) was used for peak calling of nucleosome positioning. The mapped reads in individual samples were normalized by sequencing depth in million reads. The ChIP-seq data were visualized using Integrated Genome Viewer (IGV).

Microscopy. Ndc80-GFP tagged strains were grown at 29°C and treated with thiabendazole (TBZ, 20 μg/ml) for 30 min before microscopic observation. Strains carrying a conditional β-tubulin mutation (*nda3-KM311*) were cultured at 29°C and then shifted to 16°C for 8-12 hours (labeled as 16°C). For imaging and scoring of meiotic segregation of chromosome 1 in homozygotic cells at MI anaphase or

in four-spored asci (with *cen1*-GFP), haploid strains were crossed on low-nitrogen medium (ME) and incubated at 29°C for 2 or 3 days. Images were taken using a Delta Vision Elite microscope (Applied Precision) with a 60X, 1.42 NA oil lens. Deconvolution and image projections (maximum intensity) were used for further image processing.

Spore viability. Single colonies of each diploid strain were suspended in 30 µl water, and sporulated on ME plates at 29°C for 2 or 3 days, then spread onto YES plate, and four-spored asci were separated by micromanipulation using a glass needle for dissection. The tetrads were incubated at 16°C overnight or 36°C 4 hours, and individual spores from four-spored asci were separated on the plate. The number of the total analyzed spores was scored. Plates were incubated at 26°C for 5-7 days. The number of the viable spores was scored.

Data availability. The raw and processed ChIP-seq data are deposited in the NCBI Gene Expression Omnibus (GEO) under the accession number GSE118016.

Figure S1

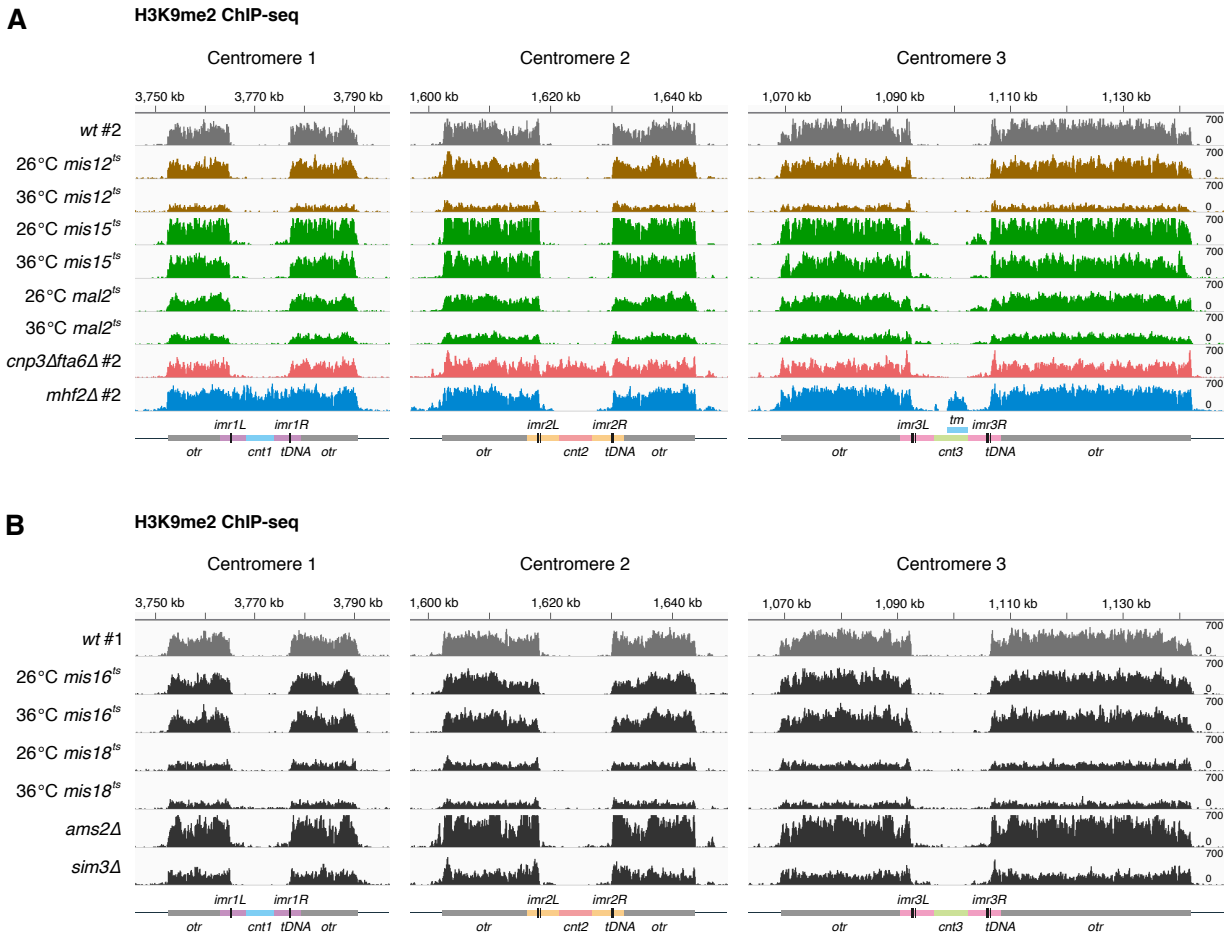

Fig. S1. *mhf2*Δ and *cnp3*Δ*fta6*Δ induce centromere inactivation. (A) H3K9me2 ChIP-seq reads mapped to centromeric and pericentromeric regions of all three chromosomes in outer kinetochore mutants (brown), inner kinetochore mutants (green), *mhf2*Δ (blue) and *cnp3*Δ*fta6*Δ (pink) compared to wild-type cells (gray). Strain names are as labeled. Cell cultures were incubated at 26°C (labeled as 26°C), or incubated at 26°C and shifted to 36°C for 6 hours (labeled as 36°C). **(B)** H3K9me2 ChIP-seq reads mapped to centromeric and pericentromeric regions of all three chromosomes in centromere-interacting mutants (black) compared to wild-type cells (gray). #1 and #2, biological replicate 1 and 2. The wild-type ChIP-seq raw data were previously published (3). Diagrams, X axis and Y axis, same as **Fig. 1.**

Figure S2

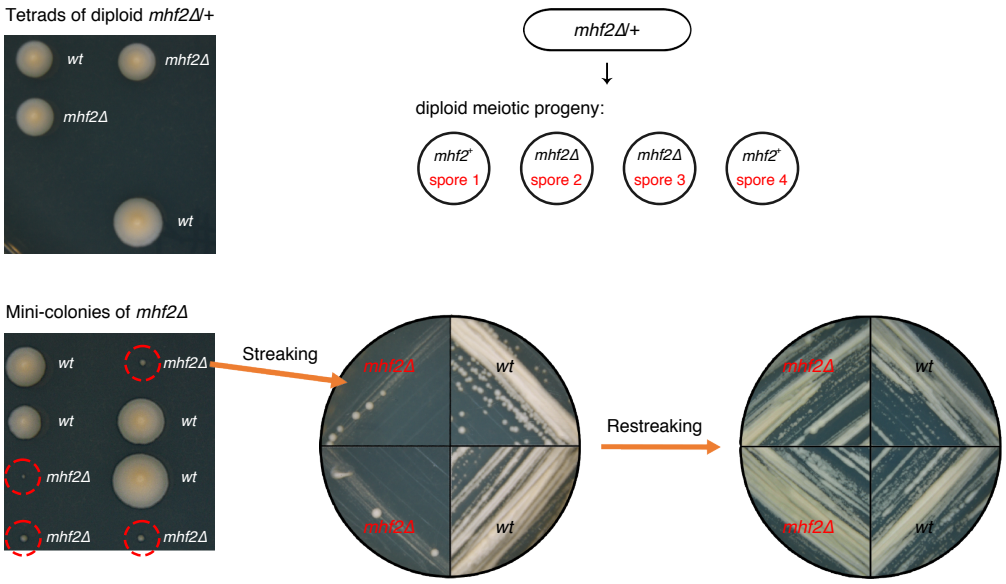

Fig. S2. The meiotic progeny of diploid *mhf2*Δ/+ have low viability. Schematic illustrates the meiotic progeny of *mhf2*Δ/+ asci. The meiotic progeny from *mhf2*Δ/+ diploid cells were dissected on a YES plate and incubated at 26°C. Mini-colonies (red dashed-line circles) from the rare *mhf2*Δ/+ asci with four viable spores were streaked on YES plates, incubated at 26°C for 6 days then re-streaked and incubated at 26°C for 6 days.

Figure S3

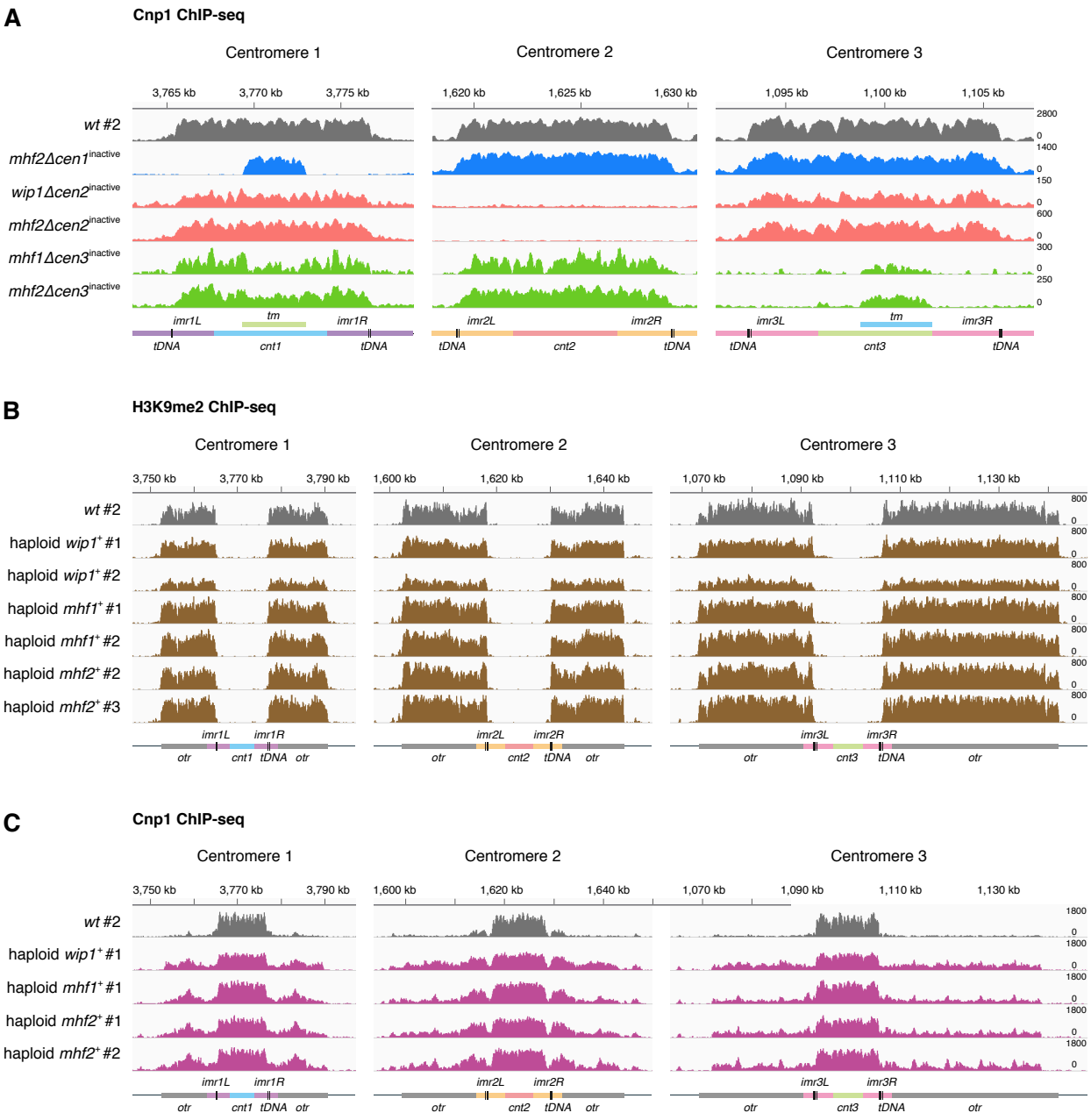

Fig. S3. Centromere inactivation occurs postzygotically and independently among *wip1*Δ, *mhf1*Δ and *mhf2*Δ meiotic progeny. (A) Cnp1 ChIP-seq reads mapped to centromeric regions of all three chromosomes in randomly chosen *wip1*Δ, *mhf1*Δ and *mhf2*Δ (*cen1*$^{\text{inactive}}$ blue, *cen2*$^{\text{inactive}}$ pink, *cen3*$^{\text{inactive}}$ green) meiotic haploid progeny compared to wild-type cells (*cen1/2/3*$^{\text{active}}$ gray). **(B)** H3K9me2 ChIP-seq reads mapped to centromeric and pericentromeric regions of all three chromosomes in the meiotic haploid progeny *wip1*$^{+}$, *mhf1*$^{+}$, *mhf2*$^{+}$ (brown) compared to wild-type cells (gray). **(C)** Cnp1 ChIP-seq reads mapped to centromeric and pericentromeric regions of all three chromosomes in the meiotic haploid progeny *wip1*$^{+}$, *mhf1*$^{+}$, *mhf2*$^{+}$ (magenta) compared to wild-type cells (gray). Tested strains were identical to that used in H3K9me2 ChIP-seq analysis as labeled in **(B).** #1 – #3, biological replicate 1 to 3. Diagrams, X axis and Y axis, same as **Fig. 1.**

Figure S4

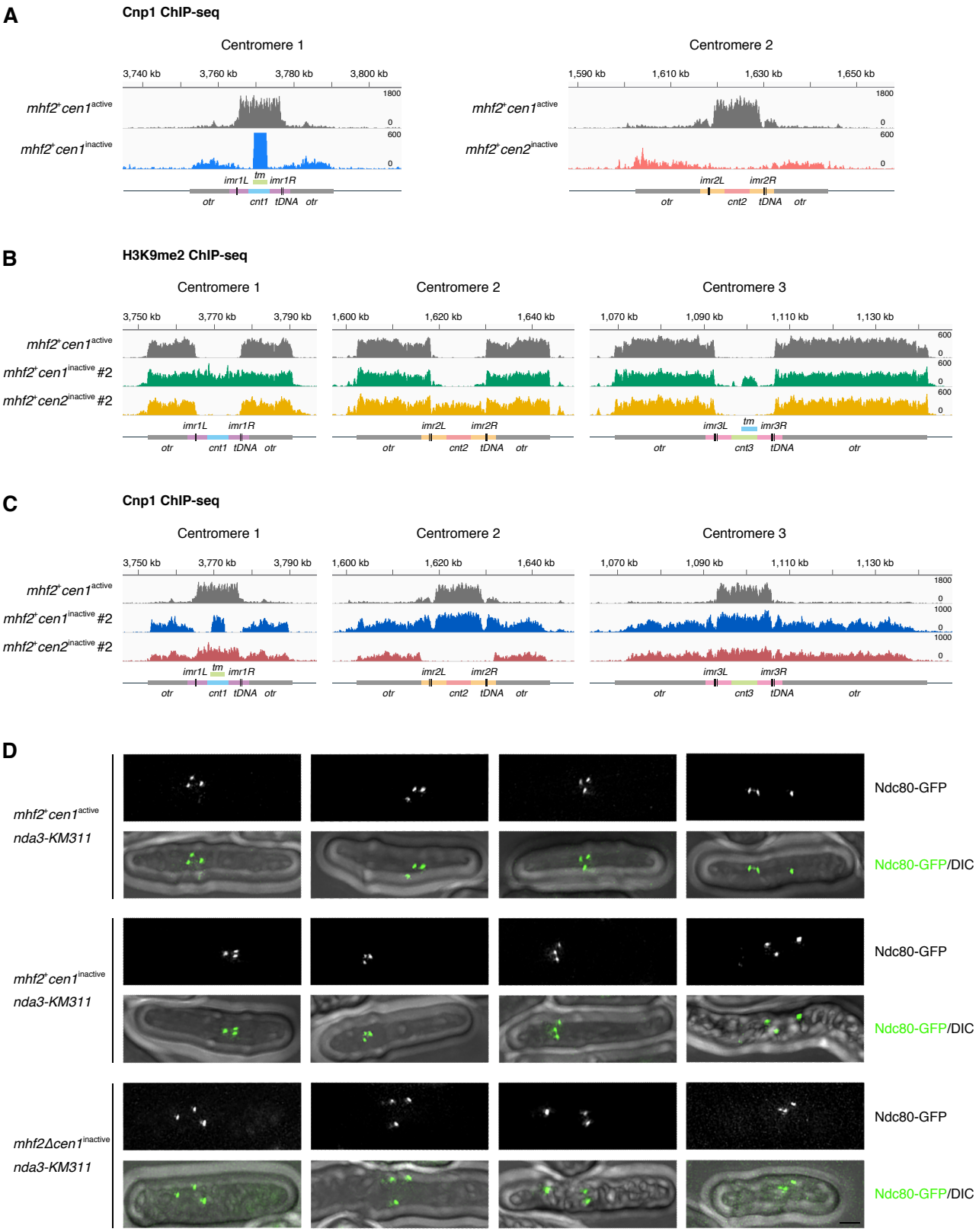
A
Cnp1 ChIP-seq
Centromere 1
3,740 kb
3,760 kb
3,780 kb
3,800 kb
mhf2+cen1active
mhf2+cen1inactive
imr1L
tm
imr1R
otr
cnt1
tDNA
otr
Centromere 2
1,590 kb
1,610 kb
1,630 kb
1,650 kb
mhf2+cen1active
mhf2+cen2inactive
imr2L
imr2R
otr
cnt2
tDNA
otr
B
H3K9me2 ChIP-seq
Centromere 1
3,750 kb
3,770 kb
3,790 kb
mhf2+cen1active
mhf2+cen1inactive #2
mhf2+cen2inactive #2
imr1L
imr1R
otr
cnt1
tDNA
otr
Centromere 2
1,600 kb
1,620 kb
1,640 kb
imr2L
imr2R
otr
cnt2
tDNA
otr
Centromere 3
1,070 kb
1,090 kb
1,110 kb
1,130 kb
imr3L
tm
imr3R
otr
cnt3
tDNA
otr
C
Cnp1 ChIP-seq
Centromere 1
Centromere 2
Centromere 3
D
mhf2+cen1active
nda3-KM311
mhf2+cen1inactive
nda3-KM311
mhf2Δcen1inactive
nda3-KM311
Ndc80-GFP
Ndc80-GFP/DIC

Fig. S4. CENP-T-W-S-X components are dispensable for the mitotic maintenance of neocentromeres. (A) "Zoomed-in" illustrations of part of **Fig. 3B** to highlight the moderate levels of Cnp1 occupancy on the inactivated centromeres. **(B)** H3K9me2 ChIP-seq reads mapped to centromeric and pericentromeric regions of all three chromosomes in *mhf2*$^{+}$*cen1*$^{\text{inactive}}$ (green) and *mhf2*$^{+}$*cen2*$^{\text{inactive}}$ (yellow) compared to wild-type cells (gray). **(C)** Cnp1 ChIP-seq reads mapped to centromeric and pericentromeric regions of all three chromosomes in identical strains *mhf2*$^{+}$*cen1*$^{\text{inactive}}$ (dark blue) and *mhf2*$^{+}$*cen2*$^{\text{inactive}}$ (dark pink) compared to wild-type cells (gray). #2, biological replicate 2. Diagrams, X axis and Y axis, same as **Fig. 1. (D)** Three dots of outer kinetochore Ndc80-GFP observed in *mhf2*$^{+}$ *cen1*$^{\text{active}}$, *mhf2*Δ*cen1*$^{\text{inactive}}$ and *mhf2*$^{+}$ *cen1*$^{\text{inactive}}$. Cells were arrested in prometaphase by conditional inactivation of β-tubulin (*nda3-KM311*) at the restrictive temperature 16°C for 10 hours. Scale bar, 2 *μm*.

Figure S5

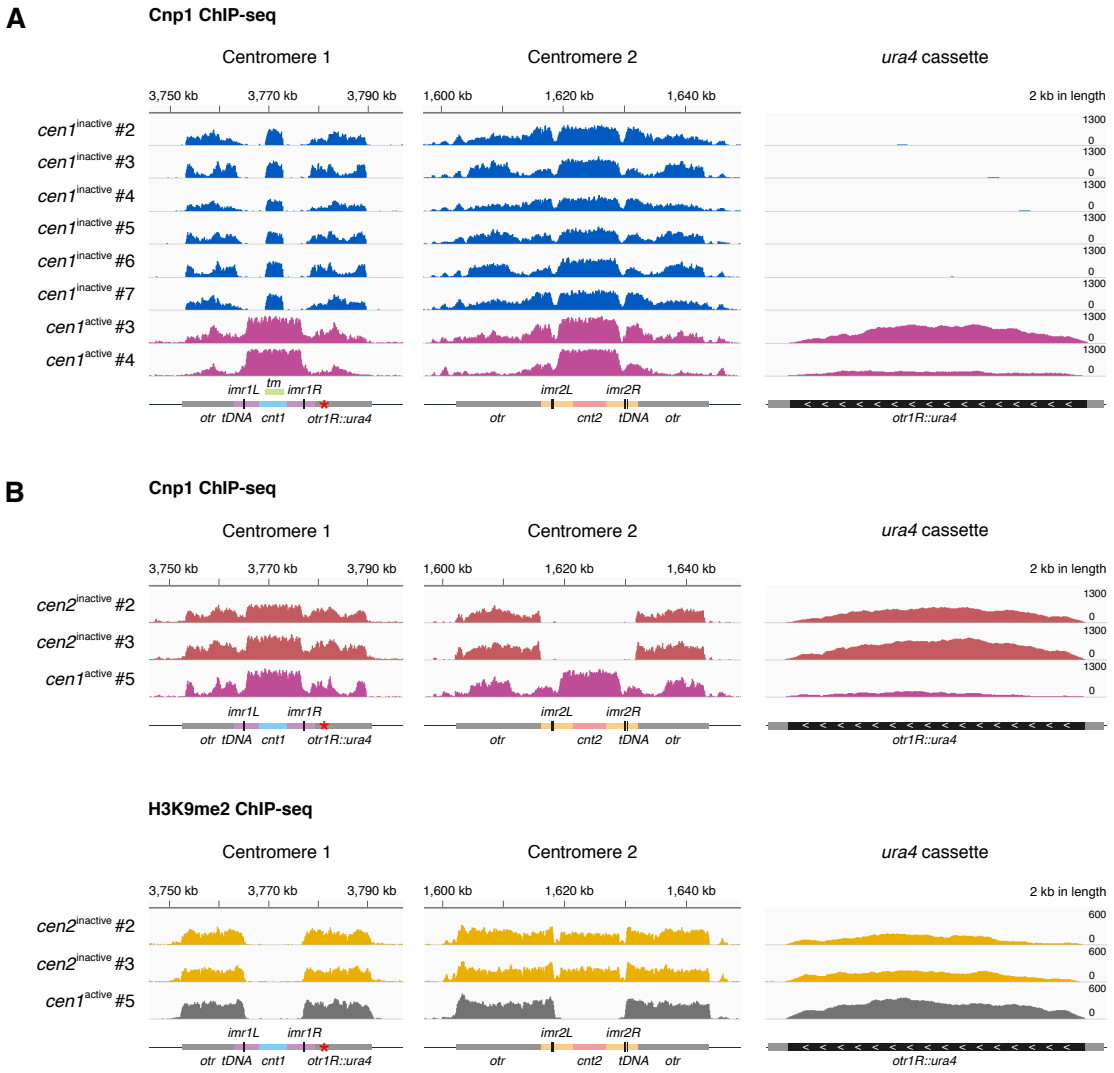

Fig. S5. Cnp1 occupancy on the pericentromeric repetitive sequences is ubiquitous and asymmetric for all three centromeres with Cnp1 spreading. (A) Cnp1 ChIP-seq reads mapped to centromeric and pericentromeric regions of all three chromosomes in *cen1*$^{\text{inactive}}$ (dark blue) and *cen1*$^{\text{active}}$ (magenta) with Cnp1 spreading. **(B)** Cnp1 ChIP-seq reads and H3K9me2 ChIP-seq reads mapped to centromeric and pericentromeric regions of all three chromosomes in *cen2*$^{\text{inactive}}$ and *cen1*$^{\text{active}}$ with Cnp1 spreading. *ura4* cassette was inserted into the right side of the *otr1R* (*otr1R::ura4*) and labeled by a red asterisk. chromosome 1, 2 and *otr1R::ura4* cassette are shown. #2 – #7, biological replicate 2 to 7. Diagrams, X axis and Y axis, same as **Fig. 1.**

Figure S6

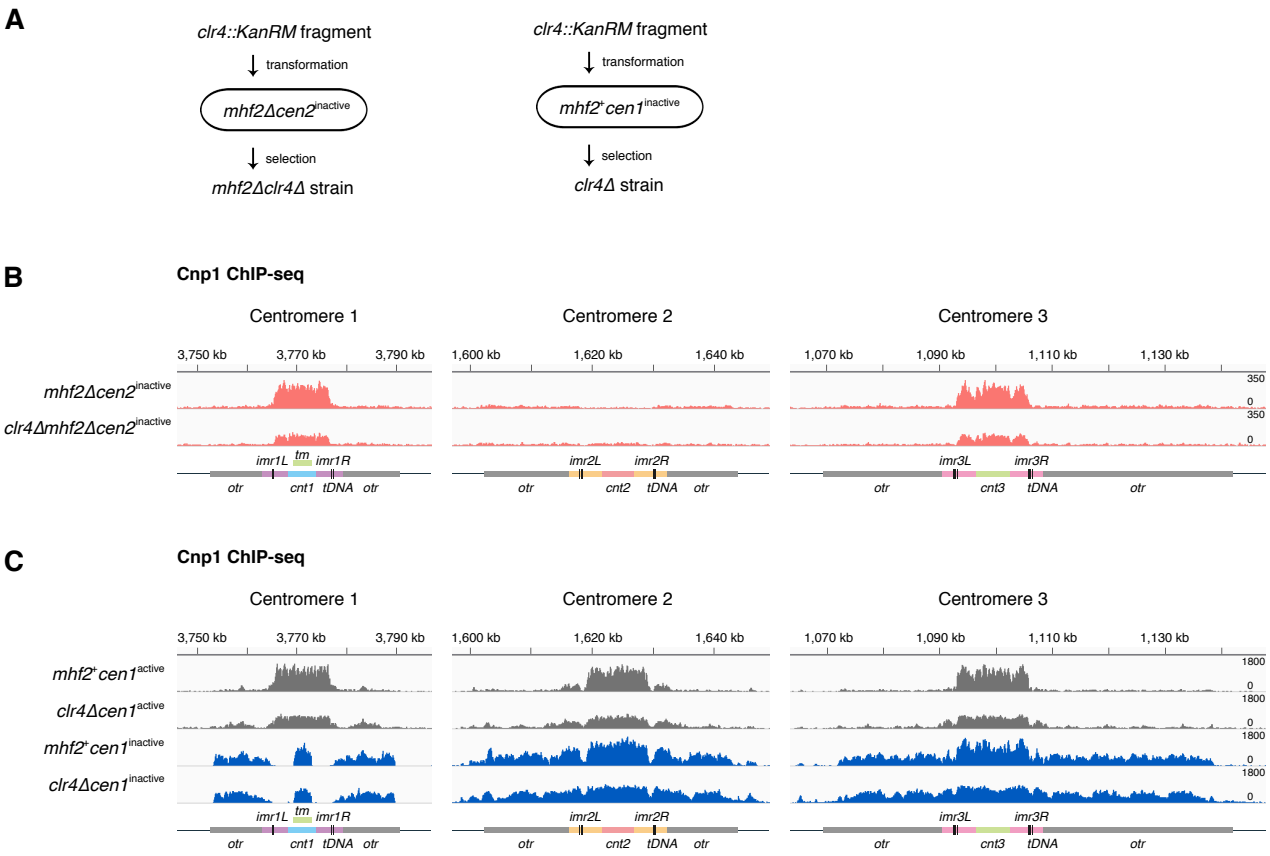

Fig. S6. Heterochromatin modification (H3K9me2) is not required for mitotic maintenance of the repositioned centromere. (A) Schematics illustrate the deletion of *clr4* in *mhf2*Δ*cen2*$^{\text{inactive}}$ (left) and *mhf2*$^{+}$*cen1*$^{\text{inactive}}$ (right) by DNA transformation. **(B)** Cnp1 ChIP-seq reads mapped to centromeric and pericentromeric regions of all three chromosomes in *mhf2*Δ*cen2*$^{\text{inactive}}$ (pink) and *clr4*Δ*mhf2*Δ*cen2*$^{\text{inactive}}$ (pink). **(C)** Cnp1 ChIP-seq reads mapped to centromeric and pericentromeric regions of all three chromosomes in *clr4*Δ*cen1*$^{\text{active}}$ (gray), *mhf2*$^{+}$*cen1*$^{\text{inactive}}$ (dark blue) and *clr4*Δ*cen1*$^{\text{inactive}}$ (dark blue) compared to *mhf2*$^{+}$*cen1*$^{\text{active}}$ wildtype (gray). Diagrams, X axis and Y axis, same as **Fig. 1.**

Figure S7

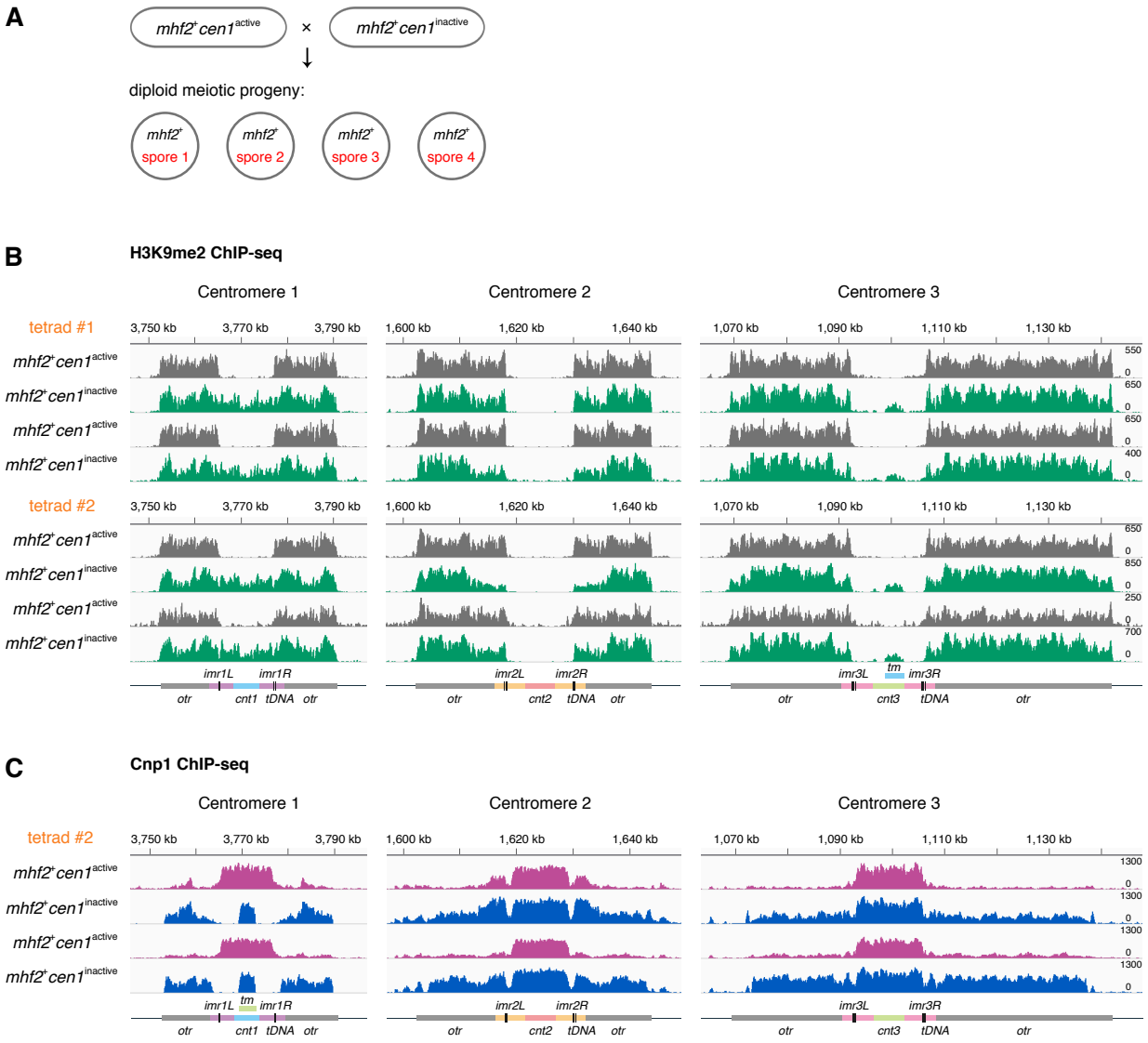

Fig. S7. The spreading of centromeric Cnp1 in *mhf2*$^{+}$*cen1*$^{\text{active}}$ is caused by *mhf2*$^{+}$*cen1*$^{\text{inactive}}$ through meiosis. (A) Schematic illustrates the meiotic progeny of *mhf2*$^{+}$*cen1*$^{\text{active}}$ × *mhf2*$^{+}$*cen1*$^{\text{inactive}}$ in asci with four spores. **(B)** H3K9me2 ChIP-seq reads mapped to centromeric and pericentromeric regions of all three chromosomes in four viable progeny from the same asci (tetrad #1 and #2). *cen1*$^{\text{inactive}}$ (green) conformed to Mendelian inheritance (2 : 2 segregation pattern). Tested strains of tetrad #1 were identical to that used in H3K9me2 ChIP-seq analysis as labeled in **Fig. 5A. (C)** Cnp1 ChIP-seq reads mapped to centromeric and pericentromeric regions of all three chromosomes in four viable progeny from the same ascus (tetrad #2). *mhf2*$^{+}$*cen1*$^{\text{inactive}}$ (dark blue) conformed to Mendelian inheritance (2 : 2 segregation pattern). *mhf2*$^{+}$*cen1*$^{\text{active}}$ (magenta) exhibited the spreading of Cnp1 into the pericentromeric regions. **SI Appendix, Fig. S7B** and **S7C** used the same strains of tetrad #2. Diagrams, X axis and Y axis, same as **Fig. 1.**

Figure S8

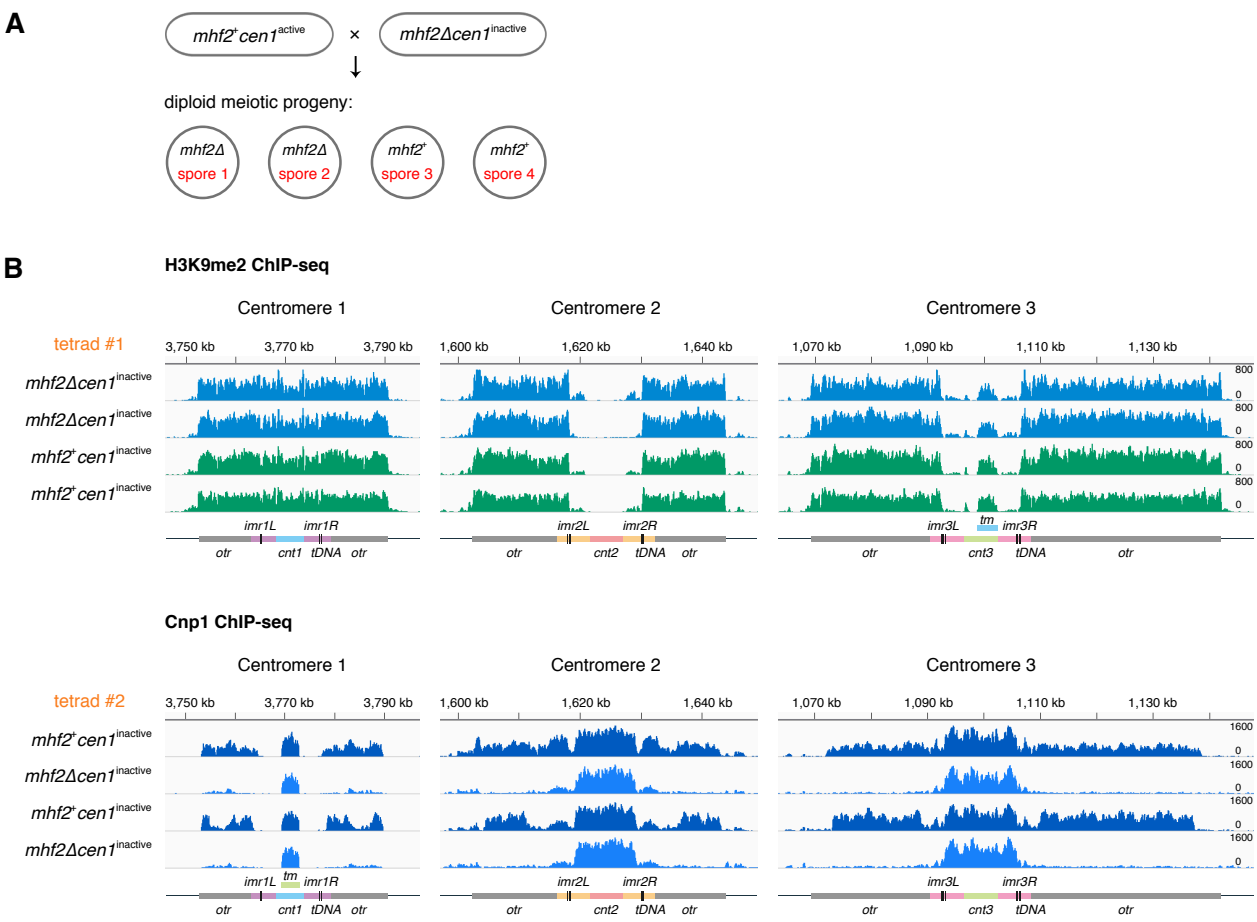
A
mhf2+ cen1active
×
mhf2Δcen1inactive
diploid meiotic progeny:
mhf2Δ spore 1
mhf2Δ spore 2
mhf2+ spore 3
mhf2+ spore 4
B
H3K9me2 ChIP-seq
Centromere 1
Centromere 2
Centromere 3
tetrad #1
mhf2Δcen1inactive
mhf2Δcen1inactive
mhf2+ cen1inactive
mhf2+ cen1inactive
3,750 kb
3,770 kb
3,790 kb
1,600 kb
1,620 kb
1,640 kb
1,070 kb
1,090 kb
1,110 kb
1,130 kb
800
0
imr1L
imr1R
otr
cnt1
tDNA
otr
imr2L
imr2R
otr
cnt2
tDNA
otr
imr3L
tm
imr3R
otr
cnt3
tDNA
otr
Cnp1 ChIP-seq
Centromere 1
Centromere 2
Centromere 3
tetrad #2
mhf2+ cen1inactive
mhf2Δcen1inactive
mhf2+ cen1inactive
mhf2Δcen1inactive
3,750 kb
3,770 kb
3,790 kb
1,600 kb
1,620 kb
1,640 kb
1,070 kb
1,090 kb
1,110 kb
1,130 kb
1600
0
imr1L
tm
imr1R
otr
cnt1
tDNA
otr
imr2L
imr2R
otr
cnt2
tDNA
otr
imr3L
imr3R
otr
cnt3
tDNA
otr

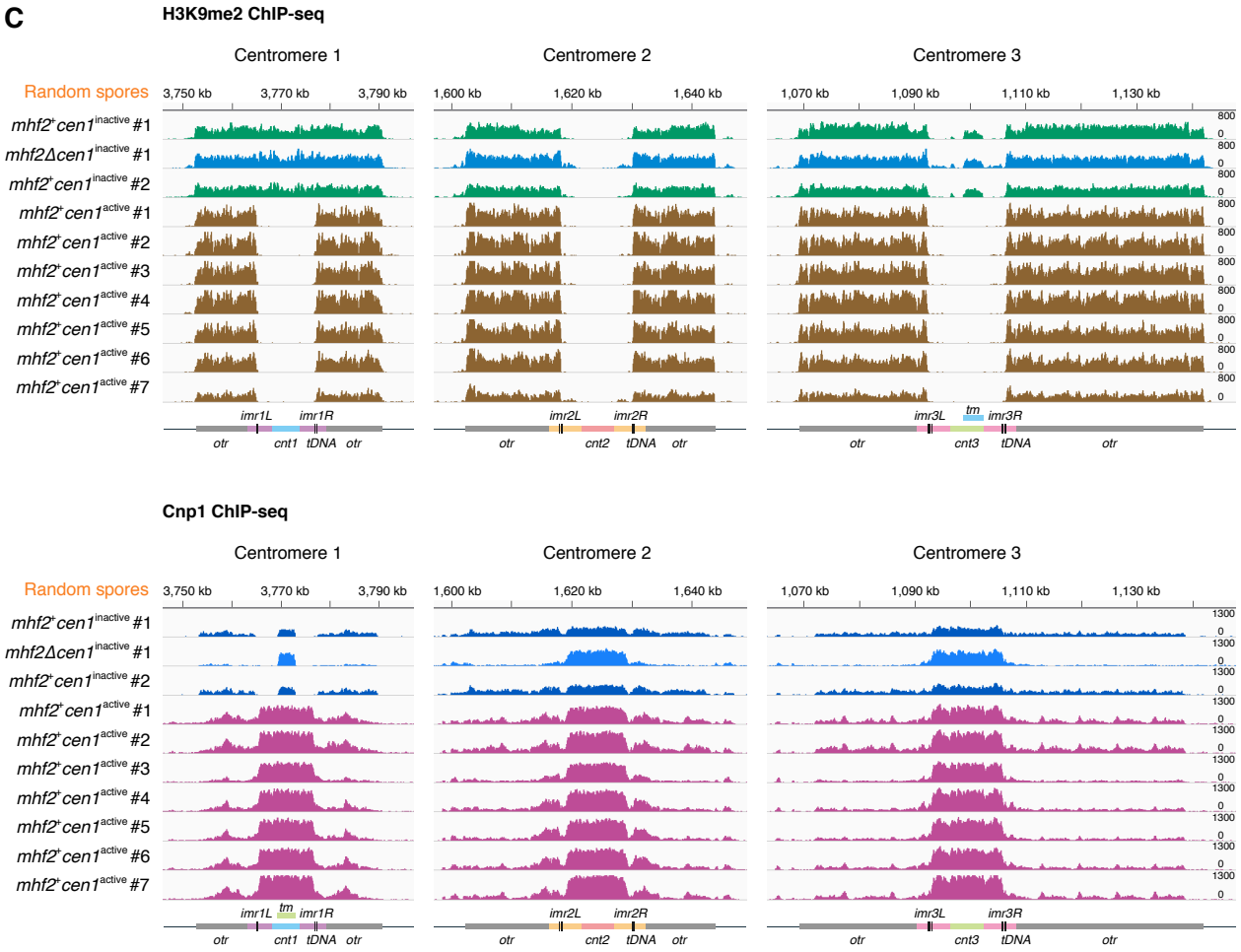

Fig. S8. *mhf2*Δ tends to convert the original centromere into an inactivated one in heterozygous meiosis. (A) Schematic illustrates the meiotic progeny of *mhf2*$^{+}$*cen1*$^{\text{active}}$ × *mhf2*Δ*cen1*$^{\text{inactive}}$ in asci with four spores. **(B)** H3K9me2 ChIP-seq reads and Cnp1 ChIP-seq reads mapped to centromeric and pericentromeric regions of all three chromosomes in four viable meiotic progeny from the tetrad #1 and #2, respectively. *mhf2*Δ conformed to Mendelian inheritance (2 : 2 segregation pattern). *cen1*$^{\text{inactive}}$ was identified. **(C)** H3K9me2 ChIP-seq reads and Cnp1 ChIP-seq reads mapped to centromeric and pericentromeric regions of all three chromosomes in randomly obtained viable meiotic progeny from *mhf2*Δ*cen1*$^{\text{inactive}}$ × *mhf2*$^{+}$*cen1*$^{\text{active}}$. Two *mhf2*$^{+}$*cen1*$^{\text{inactive}}$ were identified (#1 – #2). Seven biological replicates (#1 – #7) of *mhf2*$^{+}$*cen1*$^{\text{active}}$ (magenta) exhibited the spreading of Cnp1 into the pericentromeric regions. Diagrams, X axis and Y axis, same as **Fig. 1.**

Figure S9

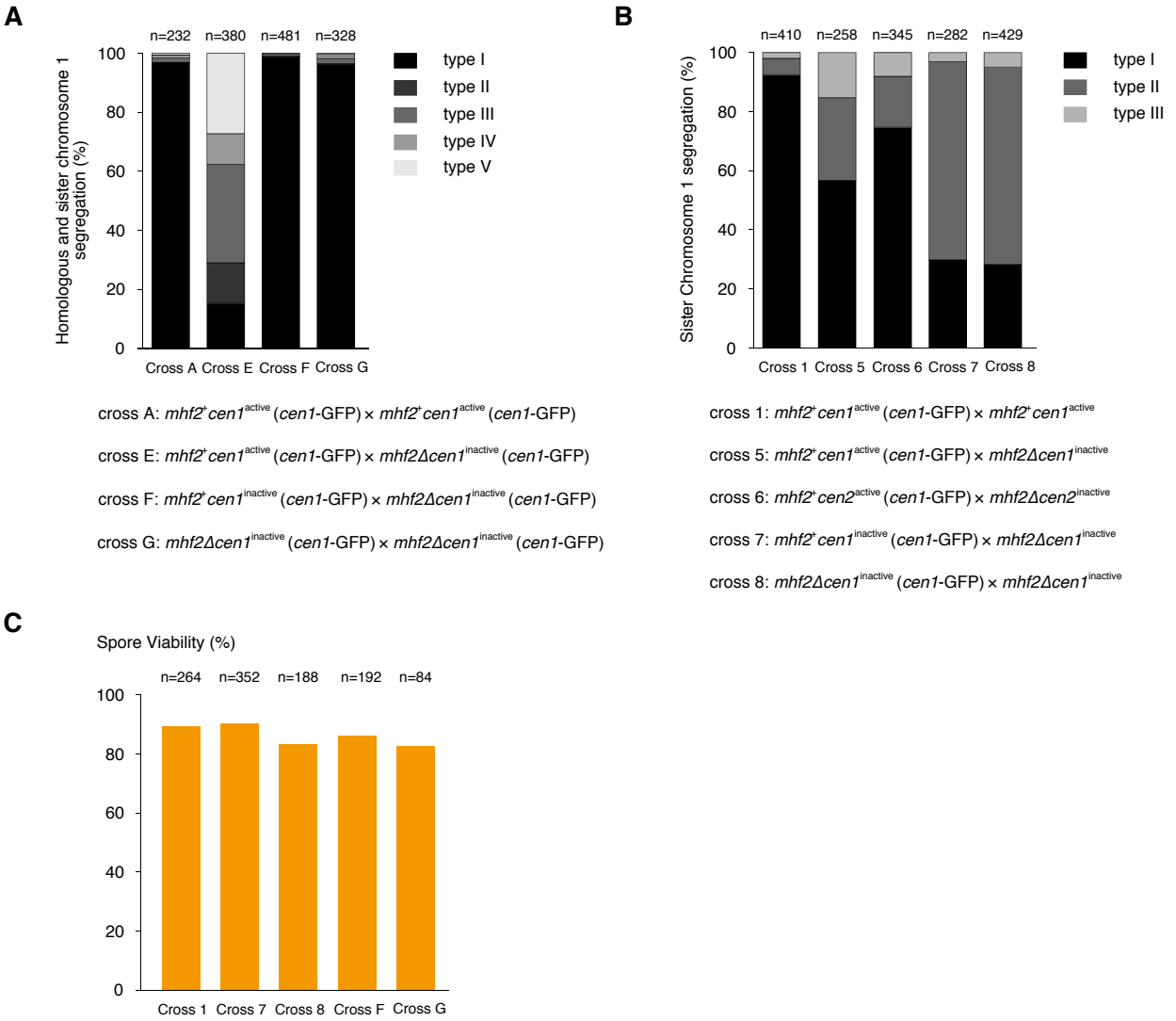

Fig. S9. Abnormal meiotic chromosome segregation accounts for the poor spore viability in heterozygotic meiosis with mismatched centromeres. (A) Both parental cells were labeled with *cen1*-GFP (green dot). The quantification of *cen1*-GFP dots distribution (type I to V) in four-spored asci of heterozygotic and homozygotic meiosis to trace the meiotic segregation of homologous chromosome 1 and sister chromosome 1. Cross A and E, *mhf2*$^{+}$*cen1*$^{\text{active}}$ cells crossed to *mhf2*$^{+}$ *cen1*$^{\text{active}}$ and *mhf2*Δ*cen1*$^{\text{inactive}}$ cells, respectively. Cross F and G, *mhf2*$^{+}$*cen1*$^{\text{inactive}}$ and *mhf2*Δ*cen1*$^{\text{inactive}}$ cells crossed to *mhf2*Δ*cen1*$^{\text{inactive}}$ cells, respectively. n, the total four-spored asci analyzed. **(B)** One of the parental cells was labeled with *cen1*-GFP (green dot). The quantification of sister *cen1*-GFP dots distribution (type I to III) in four-spored asci of heterozygotic and homozygotic meiosis to trace the meiotic segregation of sister chromosome 1. Cross 1 and 5, *mhf2*$^{+}$*cen1*$^{\text{active}}$ cells crossed to *mhf2*$^{+}$ *cen1*$^{\text{active}}$ and *mhf2*Δ*cen1*$^{\text{inactive}}$ cells, respectively. Cross6, *mhf2*$^{+}$*cen2*$^{\text{active}}$ cells carrying the *cen1*-GFP were crossed to *mhf2*Δ*cen2*$^{\text{inactive}}$ cells with mismatched *cen2*. Cross 7 and 8, *mhf2*$^{+}$*cen1*$^{\text{inactive}}$ and *mhf2*Δ*cen1*$^{\text{inactive}}$ cells crossed to *mhf2*Δ*cen1*$^{\text{inactive}}$ cells. respectively. n, the total four-spored asci analyzed. **(C)** Intact asci with four spores from the above genetic crosses were dissected microscopically and scored for the number of viable spores. Spore viability was calculated as the ratio of the number of viable spores to the number of analyzed spores. n, the total spores analyzed.

Table S1. Spore lethality is random among the meiotic progeny of diploid *wip1*Δ/+, *mhf1*Δ/+ and *mhf2*Δ/+

	Spore viability	Total dissected asci (n)	Viable deletion progeny : Viable wild-type progeny
wild type (+/+)	94.68%	47	0 : 178
*wip1*Δ/+	44.8%	48	41 : 45
*mhf1*Δ/+	48.0%	48	44 : 48
*mhf2*Δ/+	46.5%	36	35 : 32

The wild-type diploid and heterozygous deletion diploid strains were subjected to tetrad dissection. Intact asci with four spores were dissected microscopically and scored for the number of viable spores. Spore viability is calculated as the ratio of the number of viable spores to the number of analyzed spores. The number of viable deletion progeny and viable wild-type progeny were counted.

Table S2. Centromere inactivation occurs randomly in one of the three centromeres in *wip1*Δ, *mhf1*Δ and *mhf2*Δ

Genotype	Strain	*cen1*^{inactive}	*cen2*^{inactive}	*cen3*^{inactive}
*wip1*Δ	LM999	+	–	–
	LM1000	–	+	–
*mhf1*Δ	LM997	–	+	–
	LM998	–	–	+
*mhf2*Δ	LM705	+	–	–
	LM722	–	+	–
	LM732	–	+	–
	LM734	–	–	+
	LM735	–	–	+
	LM725	–	–	+

Table S3. Incompatibility between neocentromeres and original centromeres causes a meiosis barrier

Cross	Spore viability	Dissected Asci (n)	Asci with 4 viable spores	Asci with one or no viable spores	Meiosis barrier
mhf2^{+}*cen1*$^{\text{inactive}}$ × *mhf2*Δ*cen1*$^{\text{inactive}}$	91.3%	204	76%	1.96%	×
mhf2^{+}*cen1*$^{\text{inactive}}$ × *mhf2*Δ*cen2*$^{\text{inactive}}$	26.8%	291	0.34%	69.1%	√
*mhf2*Δ*cen1*$^{\text{inactive}}$ × *mhf2*Δ*cen2*$^{\text{inactive}}$	20.0%	251	0.40%	78.9%	√

Additional genetic crosses between cells with mismatched (*mhf2*$^{+}$*cen1*$^{\text{inactive}}$ × *mhf2*Δ*cen2*$^{\text{inactive}}$, *mhf2*Δ*cen1*$^{\text{inactive}}$ × *mhf2*Δ*cen2*$^{\text{inactive}}$) or matched (*mhf2*$^{+}$*cen1*$^{\text{inactive}}$ × *mhf2*Δ*cen1*$^{\text{inactive}}$) centromeres were subjected to tetrad dissection. Intact asci with four spores were dissected microscopically and scored for the number of viable spores. Spore viability is calculated as the ratio of the number of viable spores to the number of analyzed spores. > 50% reduction in spore viability is defined as meiosis barrier.

Table S4. Incompatibility between neocentromeres and original centromeres causes poor progeny viability and represents a meiosis barrier

Cross	Dissected Asci (n)	Asci with 4 viable spores	Asci with 3 viable spores	Asci with 2 viable spores	Asci with 1 viable spore	Asci with 0 viable spore
mhf2^{+}*cen1*$^{\text{active}}$ × *mhf2*$^{+}$*cen1*$^{\text{active}}$	130	80%	14.6%	3.8%	0.77%	0.77%
*mhf2*Δ*cen1*$^{\text{inactive}}$ × *mhf2*$^{+}$*cen1*$^{\text{active}}$	254	5.9%	10.6%	30.7%	29.1%	24.0%
mhf2^{+}*cen1*$^{\text{inactive}}$ × *mhf2*$^{+}$*cen1*$^{\text{active}}$	272	4.04%	1.1%	25.4%	30.5%	39.0%
mhf2^{+}*cen1*$^{\text{inactive}}$ × *mhf2*$^{+}$*cen1*$^{\text{inactive}}$#1	108	68.5%	24.1%	5.6%	1.9%	0%
mhf2^{+}*cen1*$^{\text{inactive}}$ × *mhf2*$^{+}$*cen1*$^{\text{inactive}}$#2	106	9.4%	18.9%	9.4%	12.3%	50%
mhf2^{+}*cen1*$^{\text{inactive}}$ × *mhf2*$^{+}$*cen2*$^{\text{inactive}}$	377	0.80%	4.0%	14.1%	35.8%	45.4%
mhf2^{+}*cen1*$^{\text{inactive}}$ × *mhf2*Δ*cen1*$^{\text{inactive}}$	204	76%	16.7%	5.4%	0.49%	1.47%
mhf2^{+}*cen1*$^{\text{inactive}}$ × *mhf2*Δ*cen2*$^{\text{inactive}}$	291	0.34%	4.1%	26.5%	40.6%	28.5%
*mhf2*Δ*cen1*$^{\text{inactive}}$ × *mhf2*Δ*cen2*$^{\text{inactive}}$	251	0.40%	2.0%	18.7%	35.1%	43.8%

Detailed information of all the genetic crossings in Table 1 and Table S3.

Table S5. List of *S. pombe* strains used in this study

Name	Genotype	Origin
QG323	*h+, nuf2-1, leu1-32*	National BioResource Project (Japan)
XL296	*h-, mis12-537, leu1-32*	National BioResource Project (Japan)
XL297	*h+, mis15-68, leu1-32*	National BioResource Project (Japan)
QG346	*h+, mal2-1, leu1-32*	National BioResource Project (Japan)
XL211	*h-, sim4-193, ade6-210, arg3-D4, his3-D1, leu1-32, ura4-D18*	(4)
b28-C08	*h?, fta6Δ::kanMX6, ade6Δ::hphMX6, cnt2::ade6-natMX6, leu1-32, ura4D*	*S. pombe* deletion library
b35-D11	*h?, cnp3Δ::kanMX6, ade6Δ::hphMX6, cnt2::ade6-natMX6, leu1-32, ura4D*	*S. pombe* deletion library
LM850	*h?, cnp3Δ::kanMX6, fta6Δ::kanMX6, ade6Δ::hphMX6, cnt2::ade6-natMX6, leu1-32, ura4D*	This study
LM842	*h?, cnp3Δ::KanMX6, fta6Δ::KanMX6, ade6Δ::hphMX6, cnt2::ade6-natMX6, leu1-32, ura4D*	This study
b25-E05	*h?, mhf2Δ::kanMX6, ade6Δ::hphMX6, cnt2::ade6-natMX6, leu1-32, ura4D*	*S. pombe* deletion library
LM569	*h?, mhf2Δ::kanMX6, ade6Δ::hphMX6, cnt2::ade6-natMX6, leu1-32, ura4D*	This study
QG365	*h-, mis16-53, leu1-32*	National BioResource Project (Japan)
QG366	*h-, mis18-262, leu1-32*	National BioResource Project (Japan)
XL695	*h+, ams2Δ::kanMX6*	This study
XL561	*h+, sim3Δ::kanMX6, ade6$^-$, leu1-32, ura4-D18*	This study
LW42	*h+/h-*	This study
LM702	*h+/h-, wip1Δ::natMX6/ wip1$^+$*	This study
LM700	*h+/h-, wip1Δ::natMX6/ wip1$^+$*	This study
LM701	*h+/h-, mhf1Δ::natMX6/ mhf1$^+$*	This study
LM608	*h+/h-, mhf1Δ::natMX6/ mhf1$^+$*	This study
LM599	*h+/h-, mhf2Δ::natMX6/ mhf2$^+$*	This study
LM600	*h+/h-, mhf2Δ::natMX6/ mhf2$^+$*	This study
LM982	*h?, haploid mhf2$^+$*	This study
LM971	*h?, haploid wip1$^+$*	This study
LM974	*h?, haploid wip1$^+$*	This study
LM962	*h?, haploid mhf1$^+$*	This study
LM966	*h?, haploid mhf1$^+$*	This study

LM704	*h?, haploid mhf2*$^{+}$	This study
LM985	*h?, haploid mhf2*$^{+}$	This study
LM999	*h?, haploid wip1*Δ*cen1*$^{\text{inactive}}$	This study
LM997	*h?, haploid mhf1*Δ*cen2*$^{\text{inactive}}$	This study
LM735	*h?, haploid mhf2*Δ*cen3*$^{\text{inactive}}$	This study
LM705	*h?, haploid mhf2*Δ*cen1*$^{\text{inactive}}$	This study
LM1000	*h?, haploid wip1*Δ*cen2*$^{\text{inactive}}$	This study
LM732	*h?, haploid mhf2*Δ*cen2*$^{\text{inactive}}$	This study
LM998	*h?, haploid mhf1*Δ*cen3*$^{\text{inactive}}$	This study
LM734	*h?, haploid mhf2*Δ*cen3*$^{\text{inactive}}$	This study
LM722	*h?, haploid mhf2*Δ*cen2*$^{\text{inactive}}$	This study
LM725	*h?, haploid mhf2*Δ*cen3*$^{\text{inactive}}$	This study
XL403	*h-, ndc80-GFP::kanMX6*	(5)
LM885	*h-, ndc80-GFP::kanMX6, mhf2*Δ*cen1*$^{\text{inactive}}$	This study
LM940	*h?, mhf2*Δ*cen1*$^{\text{inactive}}$	This study
LM1219	*h?, mhf2*$^{+}$*cen1*$^{\text{inactive}}$	This study
LM1144	*h?, mhf2*Δ*cen2*$^{\text{inactive}}$	This study
LM1261	*h?, mhf2*$^{+}$*cen2*$^{\text{inactive}}$	This study
LM843	*h?, mhf2*$^{+}$*cen1*$^{\text{inactive}}$	This study
LM846	*h?, mhf2*$^{+}$*cen2*$^{\text{inactive}}$	This study
LM1037	*h?, nda3-KM311, ndc80-GFP::kanMX6*	This study
LM1057	*h?, nda3-KM311, ndc80-GFP::kanMX6, mhf2*$^{+}$*cen1*$^{\text{inactive}}$	This study
LM1077	*h?, nda3-KM311, ndc80-GFP::kanMX6, mhf2*Δ*cen1*$^{\text{inactive}}$	This study
LM1080	*h?, nda3-KM311, ndc80-GFP::kanMX6, mhf2*Δ*cen1*$^{\text{inactive}}$	This study
SPT999a	*Msmt0, leu1-32, his2, ade6-210, ura4D, otr1R::ura4*$^{+}$	(6)
SPKY10	*h+, leu1-32, ade6-210, ura4D, otr1R::ura4*$^{+}$*, Asf1-TAP::KanRM*	(6)
LM1147	*h?, mhf2*$^{+}$*cen2*$^{\text{inactive}}$*, otr1R::ura4*$^{+}$	This study
LM1264	*h?, mhf2*$^{+}$*cen1*$^{\text{inactive}}$*, otr1R::ura4*$^{+}$	This study
LM1136	*h?, mhf2*$^{+}$*cen1*$^{\text{active}}$*, otr1R::ura4*$^{+}$	This study
LM1121	*h?, mhf2*$^{+}$*cen1*$^{\text{active}}$*, otr1R::ura4*$^{+}$	This study
LM1255	*h?, mhf2*$^{+}$*cen1*$^{\text{inactive}}$*, otr1R::ura4*$^{+}$	This study
LM1256	*h?, mhf2*$^{+}$*cen1*$^{\text{inactive}}$*, otr1R::ura4*$^{+}$	This study
LM1257	*h?, mhf2*$^{+}$*cen1*$^{\text{inactive}}$*, otr1R::ura4*$^{+}$	This study
LM1259	*h?, mhf2*$^{+}$*cen1*$^{\text{inactive}}$*, otr1R::ura4*$^{+}$	This study
LM1265	*h?, mhf2*$^{+}$*cen1*$^{\text{inactive}}$*, otr1R::ura4*$^{+}$	This study
LM1266	*h?, mhf2*$^{+}$*cen1*$^{\text{inactive}}$*, otr1R::ura4*$^{+}$	This study
LM1135	*h?, mhf2*$^{+}$*cen1*$^{\text{active}}$*, otr1R::ura4*$^{+}$	This study
LM1219	*h?, mhf2*$^{+}$*cen1*$^{\text{active}}$*, otr1R::ura4*$^{+}$	This study
LM1148	*h?, mhf2*$^{+}$*cen2*$^{\text{inactive}}$*, otr1R::ura4*$^{+}$	This study
LM1149	*h?, mhf2*$^{+}$*cen2*$^{\text{inactive}}$*, otr1R::ura4*$^{+}$	This study
LM1125	*h?, mhf2*$^{+}$*cen1*$^{\text{active}}$*, otr1R::ura4*$^{+}$	This study
j03-D05	*h?, clr4*Δ*::kanMX6, ade6*Δ*::hphMX6, cnt2::ade6-natMX6, leu1-32, ura4-D18*	*S. pombe* deletion library
LM1063	*h?, mhf2*Δ*clr4*Δ*cen2*$^{\text{inactive}}$*, leu1-32, ura4-D18*	This study

LM1005	*h?, clr4Δcen1*^{inactive}*, leu1-32, ura4-D18*	This study
b25-E05	*h?, mhf2Δ::kanMX6, ade6Δ::hphMX6, cnt2::ade6-natMX6, leu1-32, ura4D*	*S. pombe* deletion library
446	*h-, ade6-210, leu1-32, ura4D*	This study
447	*h+, ade6-216, leu1-32, ura4D*	This study
LM799	*h?, mhf2*$^{+}$*cen1*^{active}*, leu1-32, ura4-D18*	This study
LM800	*h?, mhf2*$^{+}$*cen1*^{inactive}*, leu1-32, ura4-D18*	This study
LM801	*h?, mhf2*$^{+}$*cen1*^{active}*, leu1-32, ura4-D18*	This study
LM802	*h?, mhf2*$^{+}$*cen1*^{inactive}*, leu1-32, ura4-D18*	This study
LM569	*h-, mhf2Δcen1*^{inactive}*, leu1-32, ura4-D18*	This study
LM570	*h-, mhf2Δcen1*^{inactive}*, leu1-32, ura4-D18*	This study
LM571	*h-, mhf2*$^{+}$*cen1*^{inactive}*, leu1-32, ura4-D18*	This study
LM572	*h-, mhf2*$^{+}$*cen1*^{inactive}*, leu1-32, ura4-D18*	This study
LM803	*h?, mhf2*$^{+}$*cen1*^{active}*, leu1-32, ura4-D18*	This study
LM804	*h?, mhf2*$^{+}$*cen1*^{inactive}*, leu1-32, ura4-D18*	This study
LM805	*h?, mhf2*$^{+}$*cen1*^{active}*, leu1-32, ura4-D18*	This study
LM806	*h?, mhf2*$^{+}$*cen1*^{inactive}*, leu1-32, ura4-D18*	This study
LM573	*h-, mhf2*$^{+}$*cen1*^{inactive}*, leu1-32, ura4-D18*	This study
LM574	*h+, mhf2Δcen1*^{inactive}*, leu1-32, ura4-D18*	This study
LM575	*h-, mhf2*$^{+}$*cen1*^{inactive}*, leu1-32, ura4-D18*	This study
LM576	*h+, mhf2Δcen1*^{inactive}*, leu1-32, ura4-D18*	This study
LM586	*h?, mhf2*$^{+}$*cen1*^{inactive}*, leu1-32, ura4-D18*	This study
LM587	*h-, mhf2Δcen1*^{inactive}*, leu1-32, ura4-D18*	This study
LM588	*h-, mhf2*$^{+}$*cen1*^{inactive}*, leu1-32, ura4-D18*	This study
LM1133	*h?, mhf2*$^{+}$*cen1*^{active}*, leu1-32, ura4-D18*	This study
LM1134	*h?, mhf2*$^{+}$*cen1*^{active}*, leu1-32, ura4-D18*	This study
LM1122	*h?, mhf2*$^{+}$*cen1*^{active}*, leu1-32, ura4-D18*	This study
LM1123	*h?, mhf2*$^{+}$*cen1*^{active}*, leu1-32, ura4-D18*	This study
LM1163	*h?, mhf2*$^{+}$*cen1*^{active}*, leu1-32, ura4-D18*	This study
LM1168	*h?, mhf2*$^{+}$*cen1*^{active}*, leu1-32, ura4-D18*	This study
LM1171	*h?, mhf2*$^{+}$*cen1*^{active}*, leu1-32, ura4-D18*	This study
QG40	*h+, cen1-GFP*	This study
QG41	*h-, cen1-GFP*	This study
LM930	*h-, cen1-GFP, mhf2Δcen1*^{inactive}	This study
LM934	*h-, cen1-GFP, mhf2*$^{+}$*cen1*^{inactive}	This study
LM1031	*h+, cen1-GFP, mhf2*$^{+}$*cen1*^{inactive}	This study
LM1243	*h+, cen1-GFP, mhf2*$^{+}$*cen2*^{inactive}	This study
LM1244	*h+, cen1-GFP, mhf2*$^{+}$*cen2*^{inactive}	This study
LM1246	*h-, cen1-GFP, mhf2*$^{+}$*cen2*^{inactive}	This study
LM1247	*h-, cen1-GFP, mhf2*$^{+}$*cen2*^{inactive}	This study

SI References

1. Kim D-U, *et al.* (2010) Analysis of a genome-wide set of gene deletions in the fission yeast Schizosaccharomyces pombe. *Nature Biotechnology* 28:617.
2. Moreno S Fau - Klar A, Klar A Fau - Nurse P, & Nurse P (1991) Molecular genetic analysis of fission yeast Schizosaccharomyces pombe. *Methods Enzymol* 194:795-823.
3. Lu M & He X (2018) Ccp1 modulates epigenetic stability at centromeres and affects heterochromatin distribution in Schizosaccharomyces pombe. *Journal of Biological Chemistry* 293(31):12068-12080.
4. Pidoux ALR, W. & Allshire RC (2003) Sim4: a novel fission yeast kinetochore protein required for centromeric silencing and chromosome segregation. *J Cell Biol* 161(2):295-307.
5. Joglekar AP, *et al.* (2008) Molecular architecture of the kinetochore-microtubule attachment site is conserved between point and regional centromeres. *J Cell Biol* 181(4):587-594.
6. Yamane K, *et al.* (2011) Asf1/HIRA facilitate global histone deacetylation and associate with HP1 to promote nucleosome occupancy at heterochromatic loci. *Mol Cell* 41(1):56-66.